Synthesis of Methylacetate in a Simulated Moving-Bed Reactor: Experiments and Modeling

Florian Lode, Gianmario Francesconi, Marco Mazzotti, and Massimo Morbidelli
ETH Swiss Federal Institute of Technology Zurich, Laboratorium für Technische Chemie,
ETH Hönggerberg, HCI F129, CH-8093 Zürich, Switzerland

Simulated moving-bed reactors (SMBR) combine chemical reaction and adsorptive separation within one single unit. Toward the design of this rather complex unit, guidelines for the proper choice of the operating parameters, that is, the flow-rate ratios and the Damköhler numbers within the different sections, have recently been devised based on a mathematical analysis of a linear-model system. For nonlinear systems, though, the influence of the operating parameters on the unit performance is less well understood. In this work, the interplay between the operating conditions and unit performance is investigated through numerical simulations and experiments, focusing on the influence of the feed stream composition. As a model system, the synthesis of methylacetate from methanol and acetic acid, catalyzed by a sulfonated ion-exchange resin, is considered. The experiments were carried out in an SMB reactor of miniplant scale. In addition, the reliability of the model predictions is evaluated by comparing the numerical simulation results with experimental data. It is shown through simulations that optimal performance is achieved where the feed to the SMBR is constituted of an equimolar mixture of the two reactants. Simulations and experimental results allow for an understanding of such a result.

Introduction

Integrated reaction–separation processes offer the potential of a substantially improved performance as compared to conventional ones (Agar, 1999). Their major advantage is given by the ability to alter the concentration profiles inside the reactor, thus influencing the degree of reactant conversion, particularly in the case of equilibrium-limited reactions. Among these operations, reactive distillation processes have gained most attention during the last years and are now established on an industrial scale for example for the synthesis of fuel oxygenates (Taylor and Krishna, 2000).

In the case of temperature-sensitive products such as pharmaceuticals or natural products, continuous reactive chromatography represents a more benign separation process, since it is based on selective adsorption rather than selective evaporation. The underlying principle is highlighted here, assuming a process in which a reactive fluid is contacted with a solid adsorbent in a countercurrent manner as shown in Figure 1 for the case of the reversible reaction $A \rightleftharpoons B + C$.

In the figure, the solid phase is conveyed at a constant flow rate from the top to the bottom of the unit, while the carrier fluid, S, is introduced at the bottom of the unit and flows upwards. The two feed ports, for the eluent and the reactant, and the two withdrawal ports, for the extract and the raffinate, subdivide the unit into four sections, as illustrated in Figure 1. As the reactant, A, is fed to the central part of the unit, a chemical reaction is triggered and the product species are formed. The more strongly adsorbing component, B, is conveyed downwards with the solid phase and is withdrawn in the extract stream, while the less retained species, C, is carried in the direction of the fluid flow, toward the raffinate outlet. Before being recycled, both the fluid and the solid phases are regenerated within sections 1 and 4. If the fluid and solid flow rates are properly adjusted, reactant A is completely consumed within the two central sections of the unit, and both products can be withdrawn at high purity with the extract and raffinate stream (Hasimoto et al., 1983; Mazzotti et al., 1996; Kawase et al., 1996, 1999; Lode et al., 2001, 2003).

Correspondence concerning this article should be addressed to M. Morbidelli.
Current address of M. Mazzotti: ETH Zürich, Institut für Verfahrenstechnik, Sonneggstrasse 3, CH-8092 Zürich, Switzerland.

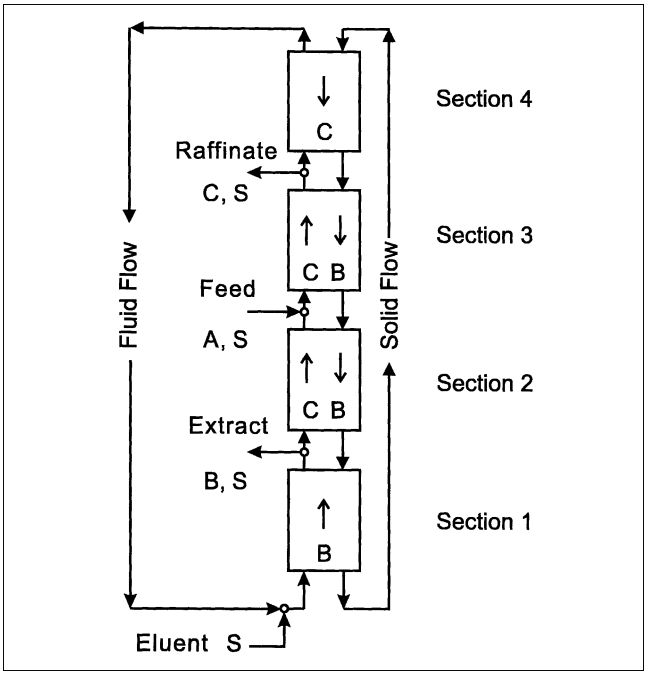

Figure 1. True countercurrent chromatographic reactor for the reaction $A \rightleftharpoons B + C$.

The practical implementation of such a true countercurrent (TCC) system is difficult, and, therefore, the simulated moving-bed process (SMB) is used, where a certain number of fixed beds are interconnected to form a closed-loop assembly and the countercurrent movement of the solid and liquid phase is simulated by periodically shifting the fluid inlets and outlets in the direction of the fluid flow, as shown in Figure 2 (Hashimoto et al., 1983; Mazzotti et al., 1996; Kawase et al., 1996, 1999; Lode et al., 2001, 2003; Ruthven and Ching, 1989).

In order to design a reactive SMB process, a detailed understanding of the dynamic behavior of a single column is necessary. The experimental and modeling procedure to be followed in order to quantitatively describe the dynamic behavior of a single reactive chromatographic column has been

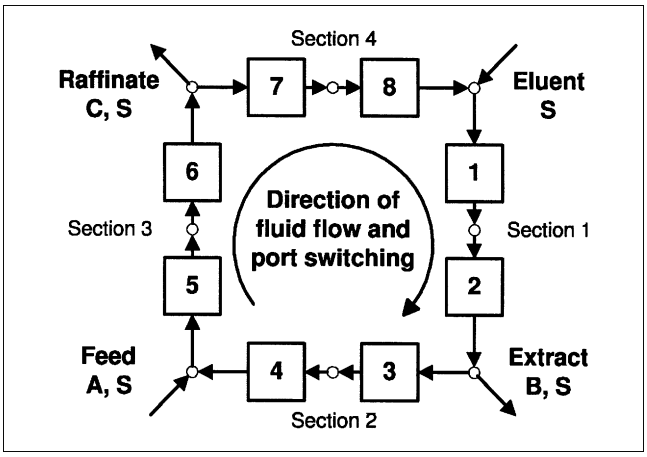

Figure 2. Simulated moving-bed reactor for the reaction $A \rightleftharpoons B + C$.

reported elsewhere (Lode et al., 2001; Mazzotti, et al., 1997). With an SMB reactor being simply the assembly of a number of such columns, the mathematical model describing one chromatographic column can be easily extended in order to simulate the SMBR unit by imposing the outlet concentration of one column as the inlet condition for the next one downstream, and by properly accounting for the additional feed or withdrawal streams. Implementing also the port-switching mechanism, the behavior of an SMBR process can be analyzed *a priori* by numerical simulation (Lode et al., 2001; Storti et al., 1988; Duennebier et al., 2000; Fricke et al., 1999).

An optimization of this rather complex process based only on numerical simulations requires extensive computations (Duennebier et al., 2000). Accordingly, shortcut design criteria have been developed recently for an idealized reaction system, $A \rightleftharpoons B + C$, with linear adsorption isotherms and mass action reaction kinetics (Lode et al., 2003). In particular, in this case, it was found that the SMBR performance is determined only by the relative flow-rate ratios of the liquid and solid phase in each section of the unit

$$m_j = \frac{Q_j t^* - \epsilon^* V_{\text{col}}}{(1-\epsilon^*)V_{\text{col}}} \tag{1}$$

by the switch time, t^*, and by the number of columns within the two central sections of the unit. In the last equation, Q_j denotes the flow rate of the liquid phase within the jth section, while V_{col} and ϵ^* represent the column volume and the total bed void fraction, respectively.

For the case of nonlinear adsorption isotherms, which are commonly encountered in practical applications, the limited capacity of the stationary phase introduces the feed concentration of the reactant as an additional parameter. While for these systems explicit shortcut design rules are still missing, a parametrical study of the unit performance based on numerical simulations can lead to the development of qualitative design guidelines, and, thus, to a more efficient design methodology (Lode et al., 2001; Fricke et al., 1999).

In this work, the performance of an SMB reactor is investigated both experimentally and through numerical simulations, using as a model system the synthesis of methyl acetate from methanol and acetic acid, catalyzed by a sulfonated ion-exchange resin. The effect of feed composition onto the qualitative and quantitative reactor performance is investigated based on a dynamic model developed previously (Lode et al., 2001). The applicability of this model is validated experimentally by comparison of the numerical predictions with the experimental results.

Experimental Setup

The SMBR unit (model C-920, Advanced Separation Technologies, Pittsburgh, PA) comprises 10 glass columns of 30-cm length and 2.5-cm internal diameter, corresponding to a volume $V_{\text{col}} = 178$ mL. Each column is packed with 68 g of Amberlyst 15 (Rohm and Haas, Philadelphia, PA) and has a total bed void fraction of $\epsilon^* = 0.65$, including a void volume of approximately 5 mL at the top of each column in order to allow for the swelling of the resin during the course of the reaction.

The inlet and outlet of each of these columns are connected to the rotating part of the valve head, while the feed and outlet streams of the unit are connected to the stationary part of the valve in a way to obtain an open-loop configuration comprising 3, 2, 3, and 2 columns in section 1, 2, 3, and 4, respectively. From pulse-tracer experiments the resulting void volume from the outlet of one column to the inlet of the next one was determined to be $V_{\text{dead}} = 7.4$ mL. The switch time of the unit was set to a value of $t^* = 10$ min for all experiments, and the unit was located within an air-conditioned laboratory leading to an operating temperature of 25 ± 2°C.

For the first two experiments technical grade methanol comprising about 0.5% mol/mol of water and 0.07% mol/mol of methyl acetate was used as the desorbent, but was exchanged for methanol of higher quality (water content of about 0.1% mol/mol, methyl acetate below the detectability limits) for all subsequent experiments. The desorbent and the extract flow rate are controlled using peristaltic pumps, while the feed stream comprising acetic acid and methanol is fed to the unit by means of a HPLC pump for better control. It is worth noting that under the operating conditions of the SMBR a variation in the fluid flow rates, $\Delta Q_j = 1$ mL/min, results in a change of the corresponding flow-rate ratio, $\Delta m_j = 0.16$, that is, a quite substantial variation as compared to the overall size of the optimum operating region, as discussed in the following. The flow rate in section 4 is set to zero in order to ensure no leakage of acetic acid, water, or methyl acetate from section 4 into section 1; accordingly a raffinate pump was not necessary.

All experiments started from the unit being equilibrated in pure methanol. The outlet streams of the unit were collected during each complete cycle (corresponding to 10 switches of the inlet and outlet ports, that is, 100 min in this case), and their average composition was analyzed by gas chromatography using a thermal conductivity detector. Steady state was assumed to be established when the difference in the experimentally determined molar amount of each of the products leaving the unit during one cycle and the molar amount of acetic acid fed to the unit within the same time interval was less than 2%. In a typical run six to eight cycles were necessary to achieve cyclic steady state, that is, between 10 and 14 h of operation.

Theoretical Analysis

The model equations and model parameters for the description of the methyl acetate synthesis in a chromatographic reactor such as the one considered here have been reported elsewhere (Lode et al., 2001).

The dynamic behavior of a single column can be described by the following mass-balance equations

$$\epsilon^* \frac{\partial c_i}{\partial t} + u_j \frac{\partial c_i}{\partial z} = \epsilon_b D_{\text{eff}} \frac{\partial^2 c_i}{\partial z^2} - (1-\epsilon^*) k_m (q_i^{\text{eq}} - q_i) \quad (2)$$

$$\frac{\partial q_i}{\partial t} = k_m (q_i^{\text{eq}} - q_i) + \nu_i r \quad (3)$$

where c_i and q_i represent the concentration of species i in the fluid and in the sorbed phase; ν_i is the corresponding stoichiometric coefficient; ϵ_b the intraparticle bed void fraction; D_{eff} the effective dispersion coefficient, calculated using the correlation given by Chung and Wen (1968); k_m the mass-transfer coefficient; t and z the space and time coordinate. The equilibrium sorbed amounts, q_i^{eq}, t and z are given by a competitive Langmuir isotherm, with water being the most strongly sorbed component, while methanol, acetic acid, and methyl acetate are less favorably sorbed. The reaction rate r is given by a mass-action expression in terms of sorbed phase concentrations (Lode et al., 2001).

In the following, the performance of the unit is investigated for different feed compositions and for a unit configuration 3–2–3–2. For all simulations, the flow rate ratios in sections 1 and 4 of the SMBR are adjusted so as to prevent any leakage of acid, ester, or water from section 1 into section 4, and vice versa. For each feed composition, the operating parameter plane spanned by the flow-rate ratios in the two central sections of the unit, m_2 and m_3, is scanned by performing numerical simulations for a large number of operating points, and by evaluating the corresponding process performance. In particular, the aim is to identify the operating conditions that lead to purities of the extract, P^E, and of the raffinate, P^R, larger than a given product specification, $P^{\min} = 0.995$, that is, where

$$P^E = \frac{n_W^E}{n_A^E + n_E^E + n_W^E} \geq P^{\min} \quad (4)$$

$$P^R = \frac{n_E^R}{n_A^R + n_E^R + n_W^R} \geq P^{\min} \quad (5)$$

Here, n_i^R ($i = A, E, W$), denotes the molar amount of acid, ester, and water, respectively, being withdrawn with the raffinate stream during one switch interval, and n_i^E applies to the extract stream.

Let us introduce the degree of conversion X of the limiting reactant, that is, acetic acid

$$X = 1 - \frac{n_A^E + n_A^R}{n_A^F} = \frac{n_E^E + n_E^R}{n_A^F} = \frac{n_W^E + n_W^R}{n_A^F} \quad (6)$$

When the purity requirements given by Eqs. 4 and 5 are fulfilled, then the following inequality for the degree of conversion can be established

$$X \geq 4P^{\min} - 3 \quad (7)$$

This can be proven by combining Eqs. 4, 5, and 6 to yield

$$\begin{aligned} 2(1-P^{\min}) &\geq \frac{n_A^E + n_E^E}{n_A^E + n_E^E + n_W^E} + \frac{n_A^R + n_W^R}{n_A^R + n_E^R + n_W^R} \\ &\geq \frac{n_A^E}{n_A^E + n_E^E + n_W^E} + \frac{n_A^R}{n_A^R + n_E^R + n_W^R} \\ &\geq \frac{n_A^E}{2n_A^F} + \frac{n_A^R}{2n_A^F} = \frac{1}{2}(1-X) \end{aligned} \quad (8)$$

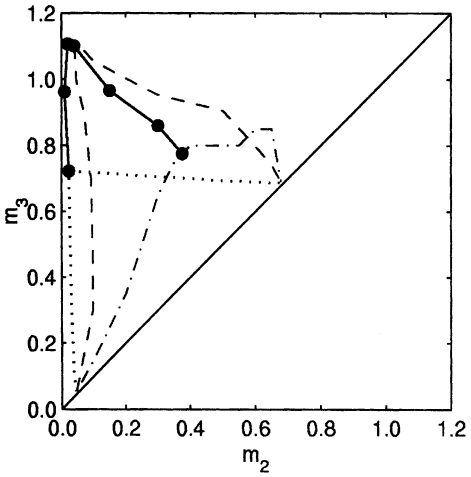

Figure 3. Effect of feed composition on process performance.

Optimum operating points (●) for feed mole fractions of acetic acid of $x_A^F = 0.01$, 0.20, 0.40, 0.50, 0.60, 0.80, and 1.00, respectively. Regions of extract and raffinate purity, P^E, $P^R \geq 0.995$, for feed mole fractions of $x_A^F = 0.01$ (dotted curve), $x_A^F = 0.50$ (dashed) and $x_A^F = 1.00$ (dash-dotted), respectively. Switch time, $t^* = 13.33$ min; flow-rate ratio section 1, $m_1 = 3$; flow-rate ratio section 4, $m_4 = -0.2$; column length, $L_{col} = 30.0$ cm; total bed void fraction, $\epsilon^* = 0.616$; unit configuration, 3–2–3–2.

Accordingly, the degree of conversion achieved for a minimum purity of $P^{min} = 0.995$ is lower bounded, that is, $X \geq X^{min} = 0.98$. Note also that the inequality in Eq. 7 is rather conservative and valid only where $P^{min} > 0.75$; it provides a valuable estimate of a lower bound for conversion only where P^{min} is rather large, that is, for high purity systems.

The operating regions, where the product specifications stated earlier are satisfied, are shown in Figure 3 for a switch time, $t^* = 13.33$ min, and the following feed mole fractions of acetic acid in methanol: $x_A^F = 0.01$ (dotted line), $x_A^F = 0.50$ (dashed), and $x_A^F = 1.00$ (dash-dotted). For the lowest acetic acid content, $x_A^F = 0.01$, the region of operating parameters leading to the required product purities is approximately given by a right triangle, which is the result expected from the analysis of the true countercurrent process in the case of linear isotherms and first-order reaction kinetics (Lode et al., 2002). In fact, there being a excess of methanol within all sections of the unit, the competitive Langmuir isotherms for acetic acid, methyl acetate, and water approach linear behavior, and the reaction rate law reduces to a linear expression in the concentration of acetic acid.

For any operating point outside this region, either the raffinate, the extract, or both outlet streams are not in accordance with the product specifications. In particular, starting from an operating point within the triangle, an increase of the flow rate ratio within section 3, m_3, leads to a shift of the concentration fronts within this section in the direction of the fluid flow, that is, toward the raffinate outlet, and eventually to a contamination of the raffinate stream by nonconverted acetic acid and nonretained water. On the other hand, for decreasing values of m_2 the concentration fronts in section 2 move toward the extract outlet, thus resulting in the breakthrough of nonconverted acetic acid and nondesorbed methyl acetate in the extract stream.

Table 1. Optimum Operating Points Leading to Purities in the Extract and Raffinate Stream P^E, $P^R \geq 0.995$ as a Function of the Mole Fraction of Acetic Acid in the Feed Stream, x_A^F

x_A^F	0.01	0.20	0.40	0.50	0.60	0.80	1.00
$m_2\|_{opt}$	0.023	0.009	0.019	0.039	0.150	0.300	0.375
$m_3\|_{opt}$	0.723	0.962	1.106	1.100	0.966	0.860	0.775

Note: Operating conditions as described in Figure 3.

It is worth noting here that for a given switch time and unit configuration the feed flow rate increases with increasing distance from the diagonal of the parameter plane (m_2, m_3). Accordingly, the maximum feed flow rate can be achieved when operating at the vertex of the triangle. In Figure 3, the optimum operating points for the case of $x_A^F = 0.01$, and for six other feed compositions ($x_A^F = 0.20$, 0.40, 0.50, 0.60, 0.80 and 1.00, respectively), are indicated by solid circles, and the corresponding coordinates are reported in Table 1. As expected, for increasing feed concentrations of acetic acid, the shape of the corresponding triangular regions, and accordingly the position of the vertex, changes. In particular, when increasing the feed mole fraction of acetic acid to $x_A^F = 0.20$, and $x_A^F = 0.40$, respectively, the vertex of the triangular region moves vertically upwards toward higher flow-rate ratios in section 3, m_3. In both cases, the boundaries of the operating region can be well approximated by straight lines (not shown here), and the base line of the respective triangles along the diagonal of the parameter plane is identical to the one found in the highly diluted case of $x_A^F = 0.01$. For $x_A^F = 0.50$ (dashed line in Figure 3), the vertex of the permissible operating region is approximately identical to the one for the case of $x_A^F = 0.40$. However, the boundaries of the triangular region now exhibit a nonlinear behavior, with both the left- and righthand boundary being bent toward the upper right-hand corner of the parameter plane. Increasing the feed mole fraction of acetic acid further from $x_A^F = 0.50$ to $x_A^F = 0.60$, 0.80, and 1.00, respectively, the vertices of the corresponding operating regions move closer toward the diagonal, and the borders of the operating regions become increasingly nonlinear. Finally, for the case of $x_A^F = 1.00$ (dash-dotted line in Figure 3) only a rather thin triangle is obtained, which is strongly skewed toward the righthand side. Nevertheless, for all feed compositions the permissible operating regions share the same intercept with the diagonal of the (m_2, m_3)-parameter plane.

A simple explanation of the effect of the feed concentration onto the qualitative shape of the operating region is difficult due to the superposition of the nonlinear sorption behavior and the nonlinear reaction kinetics. Nevertheless, some features of the behavior of the unit can be identified, and rationalized, as follows.

First, let us consider the property that for every feed concentration the intercept of the operating region with the diagonal is always the same. It is worth noting that the feed flow rate approaches zero as the distance of the operating point from the diagonal vanishes. Accordingly, the amount of acetic acid entering the unit with the feed is, under these circumstances, immediately diluted in a large amount of desorbent, namely, methanol. Since the concentrations of acetic acid, methyl acetate, and water throughout the unit remain

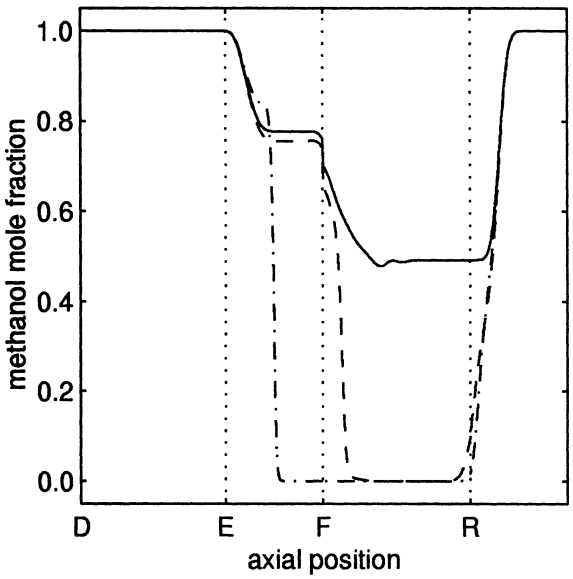

Figure 4. Concentration profiles for methanol within the unit at steady state for different feed compositions, immediately prior to the port switch.

$x_A^F = 0.60$ (solid line); $x_A^F = 0.80$ (dashed); $x_A^F = 1.00$ (dash-dotted); $m_2 = 0.25$; $m_3 = 0.75$; $t^* = 10.00$ min; unit configuration 3–2–3–2.

small, the unit behavior for any feed composition approximates that of a linear, diluted system, as explained earlier for the case of a feed concentration of $x_A^F = 0.01$.

Second, let us analyze the variations in the shape of the feasible operating region as a function of feed composition. The displacement of the vertex toward higher m_3 values for feed concentrations increasing from $x_A^F = 0.01$ to $x_A^F = 0.50$ can be explained by the more favorable sorption of acetic acid at higher concentrations. Considering that methanol is a strongly sorbed solvent as compared to acetic acid, the sorption of acetic acid is becoming more favorable for increasing acetic acid concentrations, leading to faster reaction kinetics in the sorbed phase in combination with a slower propagation velocity of acetic acid in section 3, hence with a longer residence time for the reaction.

Let us focus then on the lefthand boundary of the operating region. A significant displacement toward higher m_2 values is observed for the feed stream comprising acetic acid concentrations larger than $x_A^F = 0.50$. This phenomenon is due to the development of a zone within the central part of the reactor characterized by the absence of methanol, as can be shown by analyzing the steady-state concentration profiles inside the unit (Lode et al., 2001). As an example, in Figure 4 the methanol concentration profiles are shown for the unit operating at flow-rate ratios $m_2 = 0.25$ and $m_3 = 0.75$, and with the feed stream comprising a mole fraction of acetic acid of $x_A^F = 0.60$ (solid line), 0.80 (dashed), and 100 (dash-dotted), respectively. For the sake of comparison with the experiments, but without loss of generality, these simulations have been carried out at $t^* = 10.00$ min. Here, the mole fraction of methanol within section 1, that is, between the desorbent (D) and extract (E) port, is close to unity. Within section 2, though, methanol is contacted with acetic acid, the chemical reaction is triggered, and the mole fraction of methanol decreases. In the example, the methanol fraction decreases to values of $x_M = 0.78$ and 0.76 in the case of acetic acid feed mole fractions of $x_A^F = 0.60$ and 0.80, respectively. For a pure acetic acid feedstream ($x_A^F = 1.00$), methanol becomes the limiting reactant, and accordingly the methanol mole fraction in this case reduces to zero. Here, no additional methanol is fed to the unit in between sections 2 and 3, and accordingly there is no chemical reaction taking place within large portions of section 3. A similar behavior is observed for the case of $x_A^F = 0.80$. Here, the amount of methanol being introduced to section 3 with the feed stream is rapidly depleted by the excess amount of acetic acid, and so methanol is absent within most of section 3. Contrary to this, for $x_A^F = 0.60$ the amount of methanol entering section 3 either by convection from section 2 or with the feed is larger than the amount of acetic acid being fed, and, thus, complete consumption of methanol does not occur. In accordance with this analysis, conversion is only 0.859 and 0.541 for a feed mole fraction $x_A^F = 0.80$ and $x_A^F = 1.00$, respectively, whereas X is 0.999 when $x_A^F = 0.60$. Therefore, it can be concluded that higher flow-rate ratios, m_2, are required when $x_A^F > 0.50$ than when $x_A^F < 0.50$, where methanol can never be the limiting reagent.

Let us now consider how the process performance is affected by feed composition changes. The performance parameters to be considered are the productivity (PR), that is, the amount of methyl acetate formed per unit time and reactor volume, and the desorbent requirement (DR), that is, the amount of methanol consumed per unit amount of methyl acetate formed. In terms of the operating parameters just used, these are given by

$$PR = \frac{Q^F c_A^F X}{(1-\epsilon^*)V_{\text{unit}}} = \frac{(m_3 - m_2) X c_A^F}{n_{col} t^*} \tag{9}$$

$$DR = \frac{Q^D c_M^D + Q^F c_M^F}{Q^F c_A^F X} = \frac{(m_1 - m_4) c_M^D + (m_3 - m_2) c_M^F}{(m_3 - m_2) X c_A^F} \tag{10}$$

where c_A^F represents the volumetric concentration of acetic acid in the feed stream, which is increasing monotonically with increasing acetic acid feed mole fraction, x_A^F. For a given degree of conversion, switch time, and unit configuration, the performance of the unit is optimized by maximizing the product $(m_3 - m_2)c_A^F$, since this optimizes both PR and DR. Accordingly, for a given feed composition the optimum operating point in accordance with the purity specifications is given by the vertex of the triangle.

The optimum productivity and desorbent consumption for the feed compositions investigated earlier are plotted in Figure 5 vs. the acetic acid feed mole fraction. Starting from infinite dilution conditions (in practice $x_A^F = 0.01$), the maximum feed flow rate is increasing for feed concentrations of acetic acid of $x_A^F = 0.20$, 0.40, and 0.50, respectively, as already noted and discussed with reference to Figure 3. The productivity of the process is thus increasing strongly due to the combination of higher feed flow rates and higher acetic acid feed concentrations. For a feed mole fraction of acetic acid of approximately $x_A^F = 0.50$, the permissible feed flow

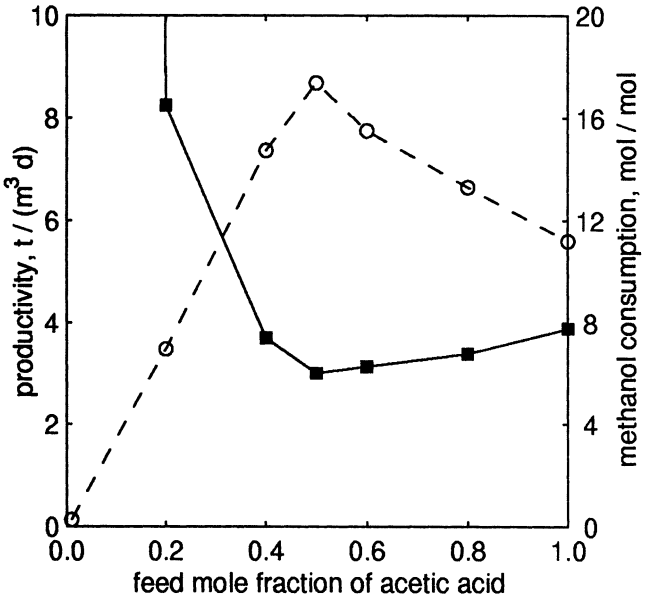

Figure 5. Unit productivity (○) and methanol consumption (■) as a function of the mole fraction of acetic acid in the feed stream.

Operating conditions as described in Figure 3.

rate exhibits a maximum, and then it decreases for larger feed concentrations. In terms of productivity, though, the effect of reducing feed flow rates can partly be counterbalanced by the increase in the feed concentration of acetic acid. Quantitatively, a maximum productivity of about 8.5 tons of methyl acetate per cubic meter of reactor volume per day is achieved for an equimolar mixture of the two reactants in the feed stream.

Considering the amount of methanol consumed in the process, low feed concentrations lead to excessively high desorbent requirements due to the large amount of additional methanol being fed with the feed stream. For feed streams of higher acid concentration, though, the solvent consumption reduces drastically, until a minimum value of about 6.0 moles of methanol to be fed to the unit per mole of acetic acid is found at a feed mole fraction of acetic acid $x_A^F = 0.50$. As the achievable feed flow rates decrease for increasing the feed concentration further, the improvement in the feed concentrations cannot counterbalance the detrimental effect on the eluent consumption, and the desorbent consumption increases toward the limit of pure acetic acid being fed to the unit.

To summarize, it was found that a feed composition comprising of a nearly stoichiometric mixture of acetic acid and methanol leads to the optimum performance of the unit both in terms of productivity and eluent consumption. In order to demonstrate that this result is of general validity for SMBRs, though, additional work has to be done, concentrating on reactive systems with different sorption characteristics and different reaction stoichiometry.

Experimental Study

The operating parameters for each of the eight experiments presented here are reported in Table 2, together with the compositions of the outlet streams under steady-state operation. The location of the corresponding operating points in the m_2, m_3 parameter plane is shown in Figure 6, together with the operating region leading to purities of the outlet streams higher or equal to $P^{\min} = 0.995$, as calculated through numerical simulations for the case where the feed is pure acetic acid, namely, $x_A^F = 1$ and $t^* = 10.00$ min, as in the experimental runs.

Due to the presence of significant amounts of dead volume, V_{dead}, in the experimental plant, the flow-rate ratio parameters, m_j, are modified here in order to account for the reduction in the net flow rate of the liquid phase due to the shifting of liquid confined within these void volumes

$$m_j^{\text{eff}} = \frac{Q_j t^* - \epsilon^* V_{\text{col}} - V_{\text{dead}}}{(1-\epsilon^*)V_{\text{col}}} \tag{11}$$

While the applicability of this approach has been demonstrated for the case of nonreactive SMB-applications (Migliorini et al., 1999), the situation encountered in reactive SMB processes is more complex. In particular, the presence of void volumes has an impact on the reactor's residence-time distribution, and, therefore, on the degree of conversion. Given that the void volume in this investigation accounts for only 4% of the total volume, this effect is considered to be negligible. In the case of larger amounts of dead volume, a detailed investigation of the effect of void volumes on the

Table 2. Operating Parameters and Performance of the SMBR Experimental Runs

	Operating Parameters			Extract Composition				Raffinate Composition			
Run	m_1^{eff}	m_2^{eff}	m_3^{eff}	x_E^E [%]	x_W^E [%]	x_A^E [%]	P_W^E	x_E^R [%]	x_W^R [%]	x_A^R [%]	P_E^R
1	1.86	0.32	0.52	0.08	8.43	0.00	0.991	6.29	1.83	0.00	0.775
2	3.79	0.27	0.48	0.07	4.64	0.00	0.985	6.22	0.63	0.00	0.908
3	3.68	0.49	0.65	0.00	2.86	0.00	1.000	4.77	0.43	0.00	0.917
4	3.65	0.43	0.73	0.00	6.28	0.00	1.000	8.64	0.36	0.00	0.960
5	3.74	0.39	0.86	0.00	5.86	0.00	1.000	13.09	0.36	0.23	0.957
6	3.64	0.18	0.66	0.00	9.27	0.00	1.000	13.69	1.15	0.00	0.923
7	3.48	0.24	0.73	0.01	10.34	0.00	0.999	12.10	0.44	0.12	0.956
8	3.59	0.22	0.71	0.02	6.25	0.00	0.997	9.36	0.50	0.00	0.949

Note: Includes m_j^{eff} parameters, as well as raffinate and extract composition and purity at steady state; switch time, $t^* = 10.00$ min; feed stream comprising pure acetic acid except for run 7 ($x_A^F = 0.80$) and run 8 ($x_A^F = 0.60$). Methanol of a higher grade was used in runs 3 to 8 (water content of about 0.1% mol/mol, and methyl acetate below the detectability limits).

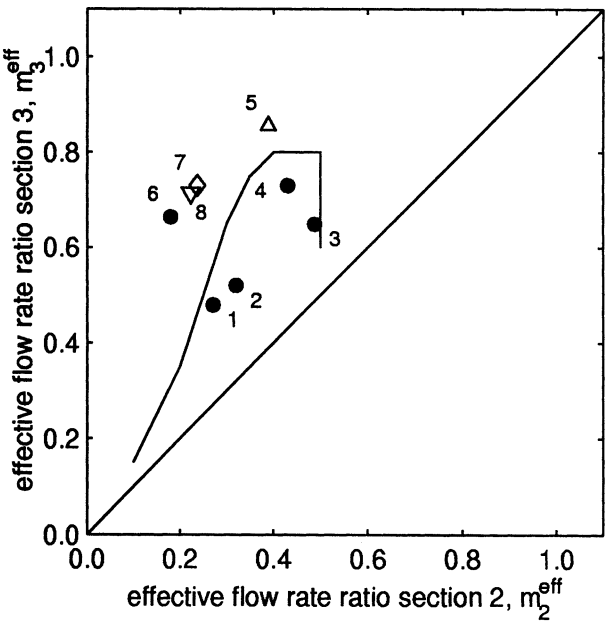

Figure 6. Operating points of the experimental runs summarized in Table 2 and operating region leading to extract and raffinate purities $P \geq 0.995$ as predicted by the numerical simulations (solid line; $t^* = 10.00$ min; $x_A^F = 1.00$; unit configuration 3–2–3–2).

Experimental data: complete conversion, partial contamination of raffinate stream by water due to incomplete regeneration (●); contamination of raffinate stream by unconverted acetic acid (△); contamination of extract stream by methyl acetate (▽); arabic numbers indicate the number of the experiment as described in Table 2.

performance of an SMBR is necessary; its implementation in the simulation code, however, would be straightforward (Migliorini et al., 1999).

Before investigating the effect of the flow rates within sections 2 and 3 of the SMBR, the necessary experimental conditions necessary to properly displace any sorbed amounts of water from the resin in section 1 have to be identified. Here, runs 1 and 2 were performed at identical flow conditions within sections 2 and 3, but with different fluid flow rates in section 1. In particular, the desorbent flow rate in section 1 was increased from $Q_1 = 23.9$ mL/min for run 1 to $Q_1 = 35.9$ mL/min for run 2, corresponding to $m_1 = 1.86$ (run 1) and $m_1 = 3.79$ (run 2), respectively. In the first case, significant amounts of water are present in the raffinate stream. As the absence of unconverted acetic acid in the raffinate indicates complete conversion within the central sections of the unit, this amount of water originates from the incomplete regeneration of the resin in section 1. Upon increasing the flow-rate ratio in section 1, the desorption of water is improved, and accordingly the amount of water present in the raffinate is substantially reduced (run 2). In addition, for this experiment the water concentrations at the inlet and outlet of the first column of section 1 at the end of a switch interval were identical, and less than 0.1%. This implies that a further improvement in resin regeneration can only be obtained by using methanol of higher grade, that is, with a lower water content, as the desorbent, making any further increase of the flow rate ratio in section 1 useless. In fact, methanol with a water content of about 0.1% mol/mol, and methyl acetate below the detectability limits was used for experimental runs 3 to 8.

After identification of the operating conditions for proper regeneration, the effect of the feed flow rate onto the performance of the unit was investigated. In particular, the feed flow rate was increased from $Q^F = 1.0$ mL/min (run 3) to $Q^F = 1.9$ mL/min (run 4) and $Q^F = 2.9$ mL/min (run 5), respectively, keeping the fluid flow rate in sections 1 and 2 constant at about $Q_1 = 35.3$ mL/min and $Q_2 = 15.0$ mL/min, respectively. Within the (m_2, m_3) parameter plane, these operating points belong to a straight line, which is almost vertical, as can be seen in Figure 6. In run 3, complete conversion of acetic acid has been achieved. While the extract comprises only water and methanol, the raffinate stream contains small amounts of water besides methyl acetate, leading to a raffinate purity $P^R = 0.917$. The same behavior is found when operating the unit with a feed flow rate approximately twice as high (run 4); with the extract again being completely pure, the raffinate purity is improved to $P^R = 0.960$, due to the larger amount of methyl acetate formed. It is worth noting, that under these conditions acetic acid also could be detected in neither the extract nor in the raffinate stream. Upon further increasing of the feed flow rate, though, the time available for reaction within the central sections of the unit is too short to allow for the complete conversion of acetic acid, and accordingly traces of acetic acid are leaking into the raffinate stream in run 5.

Furthermore, the effect of feed composition onto the performance of the reactive SMB unit was investigated. In particular, the focus was on experimentally validating the occurrence of zones of complete methanol depletion within the unit, which had been indicated by the numerical simulations for operating conditions corresponding to low fluid flow rates in section 2, and high feed flow rates. Here, such conditions are realized in runs 6 to 8, where the effluent streams of each of the individual columns of the unit were sampled close to the end of a switch interval at cyclic steady state. The corresponding concentration profiles for methanol are shown in Figure 7. In run 6, operating at pure acetic acid feed ($x_A^F = 1.00$; ● in Figure 7), the mole fraction of methanol in the liquid phase decreases from $x_M = 0.91$ at the outlet of column 3 to $x_M = 0.015$ at the outlet of column 5, that is, the last column of section 2. This is in remarkably good agreement with the model simulations reported in Figure 4 (dash-dotted line), and can be explained in the same manner.

The complete consumption of methanol within section 2, and the corresponding detrimental effect on unit performance, can be prevented by introducing additional methanol with the feedstream. Therefore, runs 7 and 8 have been performed at operating conditions similar to run 6, but with different feed compositions. For 20% of methanol in the feedstream $x_A^F = 0.80$; ▼ in Figure 7), substantial amounts of methanol are consumed by the chemical reaction in section 2, just as in the case of the pure acetic acid feed. The minimum mole fraction of methanol throughout the unit, though, never decreases below $x_M = 0.17$. By further increasing the amount of methanol in the feed stream (run 8, $x_A^F = 0.60$; ■ in Figure 7), the methanol concentrations within the unit remain above $x_M = 0.50$, thus letting acetic acid be the limiting reactant throughout the entire unit.

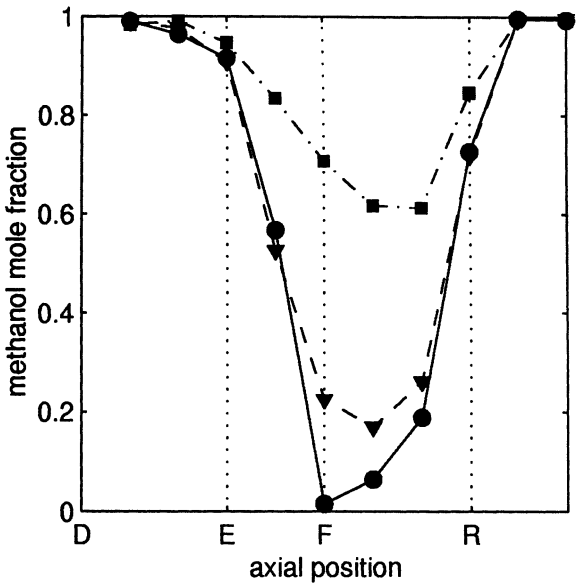

Figure 7. Concentration profiles for methanol within the unit at steady state for different feed compositions, immediately prior to the column movement.

$x_A^F = 1.00$ (run 6, ●); $x_A^F = 0.80$ (run 7, ▼); $x_A^F = 0.60$ (run 8, ■).

Thus summarizing, it can be concluded that when comparing the experimentally observed qualitative performance of the unit with the predictions obtained from the modeling analysis, a satisfactory agreement is found. In particular, the operating points for runs 2 to 4 are numerically predicted to lead to a conversion of acetic acid in excess of $X^{\min} = 0.98$, and in fact complete conversion is achieved in the experiments. Furthermore, it was experimentally confirmed that the feed flow rate adopted in run 5 is slightly too high to allow for a complete conversion. Although a more detailed experimental study is advisable in order to challenge the numerical predictions more, it can be concluded that the model describes the behavior of the unit in a satisfactory manner. Considering the behavior of the unit for different feed compositions, it has been shown experimentally that for certain operating conditions, zones devoid of methanol occur in section 2. This behavior is again in rather good agreement with the modeling analysis, and, thus, the validity of the model is further supported.

Conclusions

The effect of the feed composition on the performance of a simulated moving-bed reactor (SMBR) has been investigated based on numerical simulations for the case of a bimolecular reaction characterized by nonlinear adsorption thermodynamics of the involved chemical species. In particular, the operating regions leading to product streams of a certain purity specification have been investigated for different feed compositions, and the observed variations have been rationalized on a qualitative basis. Quantitatively, feed compositions composed of approximately an equimolar mixture of both reactants have been found through simulations to result in optimum process performance in terms of productivity and eluent consumption. In addition, the applicability of the process model to design and optimize SMBR operation was assessed through an experimental investigation of the methylacetate synthesis on Amberlyst 15 using an SMBR of miniplant scale. The experimental results are consistent with the simulations, particularly as regards the effect of feed composition on process performance and internal composition profiles.

Acknowledgments

Financial support by Roche AG, Sisseln, Switzerland, and scientific discussions with Mr. J. Jeisy and Dr. J. R. Herguijuela are gratefully acknowledged.

Notation

c_i = liquid-phase concentration
D_{eff} = axial dispersion coefficient
DR = desorbent requirement
k_m = mass-transfer coefficient
n_i = molar amount
n_{col} = number of columns of SMBR unit
m_j = flow-rate ratio
P = purity
PR = productivity
q_i = adsorbed-phase concentration
Q_j = volumetric fluid flow rate
r = reaction rate
t = time coordinate
t^* = switch time
u_j = superficial fluid velocity
V_{col} = column volume
V_{dead} = extracolumn dead volume
x_i = liquid-phase mole fraction
X = conversion
z = space coordinate

Greek letters

ϵ^* = total bed void fraction
ϵ_b = bed void fraction
ν_i = stoichiometric coefficient

Superscripts and subscripts

D = desorbent stream
E = methyl acetate, and extract stream
eff = accounting for extra-column dead volume
eq = at equilibrium
F = feed stream
min = minimum requirement from product specifications
R = raffinate stream
A = acetic acid
E = methyl acetate
i = ith component
j = jth section
M = methanol
W = water

Literature Cited

Agar, D. W., "Multifunctional Reactors: Old Preconceptions and New Dimensions," *Chem. Eng. Sci.*, **54**, 1299 (1999).

Chung, S. F., and C. Y. Wen, "Longitudinal Dispersion of Liquid Flowing Through Fixed and Fluidized Beds," *AIChE J.*, **17**, 857 (1968).

Duennebier, G., F. Fricke, and K.-U. Klatt, "Optimal Design and Operation of Simulated Moving Bed Chromatographic Reactors," *Ind. Eng. Chem. Res.*, **39**, 2290 (2000).
Fricke, J., M. Meurer, J. Dreisörner, and H. Schmidt-Traub, "Effect of Process Parameters on the Performance of a Simulated Moving Bed Chromatographic Reactor," *Chem. Eng. Sci.*, **54**, 1487 (1999).
Hashimoto, K., S. Adachi, H. Noujima, and Y. Ueda, "A New Process Combining Adsorption and Enzyme Reaction for Producing Higher-Fructose Syrup," *Biotechnol. Bioeng.*, **25**, 2371 (1983).
Kawase, M., T. B. Suzuki, K. Inoue, K. Yoshimoto, and K. Hashimoto, "Increased Esterification Conversion by Application of the Simulated Moving Bed Reactor," *Chem. Eng. Sci.*, **51**, 2971 (1996).
Kawase, M., Y. Inoue, T. Araki, and K. Hashimoto, "The Simulated-Moving-Bed Reactor for Production of Bisphenol A," *Catal. Today*, **48**, 199 (1999).
Lode, F., M. Houmard, C. Migliorini, M. Mazzotti, and M. Morbidelli, "Continuous Reactive Chromatography," *Chem. Eng. Sci.*, **56**, 269 (2001).
Lode, F., M. Mazzotti, and M. Morbidelli, "Comparing True Countercurrent and Simulated Moving-Bed Chromatographic Reactors," *AIChE J.*, **49**, 977 (2003).
Mazzotti, M., A. Kruglov, B. Neri, D. Gelosa, and M. Morbidelli, "A Continuous Chromatographic Reactor: SMBR," *Chem. Eng. Sci.*, **51**, 1827 (1996).
Mazzotti, M., B. Neri, D. Gelosa, and M. Morbidelli, "Dynamics of a Chromatographic Reactor: Esterification Catalyzed by Acidic Resins," *Ind. Eng. Chem. Res.*, **36**, 3163 (1997).
Migliorini, C., M. Mazzotti, and M. Morbidelli, "Simulated Moving Bed Units with Extracolumn Dead Volume," *AIChE J.*, **45**, 1411 (1999).
Ruthven, D. M., and C. B. Ching, "Counter Current and Simulated Counter Current Adsorption Separation Processes," *Chem. Eng. Sci.*, **44**, 1011 (1989).
Storti, G., M. Masi, R. Paludetto, M. Morbidelli, and S. Carrá, "Adsorption Separation Processes: Countercurrent and Simulated Countercurrent Operations," *Comput. Chem. Eng.*, **12**, 475 (1988).
Taylor, R., and R. Krishna, "Modeling Reactive Distillation," *Chem. Eng. Sci.*, **55**, 5183 (2000).

Manuscript received July 12, 2002, and revision received Dec. 9, 2002.